Article type: Article

Title Oxidation-Led Decomposition of Hexagonal Boron Nitride Coatings on Alloy Substrates at 900°C: Ti-6Al-4V

Christopher Fleming

Advanced Forming Research Centre, The Department of Design, Manufacture and Engineering Management, University of Strathclyde, 85 Inchinnan Drive, Inchinnan, Renfrewshire, PA4 9LJ, UK

christopher.fleming@strath.ac.uk

Hexagonal boron nitride (h-BN) coatings on Ti-6Al-4V substrates undergo complete decomposition in air at 900°C. This fate is similar to that of this ceramic material on chromia-former alloys, and unlike that of a mass of powder treated in isolation. As the ceramic and alloy oxidise concurrently, outwardly diffusing aluminium (III) ions but not the predominant titanium (IV) ions react with the boron trioxide that forms around the h-BN basal plane peripheries. Resultant aluminium borate is incorporated into the growing scale and the boron trioxide diffusion barrier is depleted. By this mechanism, the oxidation of h-BN is maintained at an enhanced rate, until both this material and its oxide completely decompose. Liberated nitrogen from the oxidation of h-BN can enter the underlying scale as a randomly distributed solute in rutile solid solution. The post-coating oxide-atmosphere interface comprises elongated aluminium borate crystallites protruding through at the boundaries between 3-5

at.% nitrogen-doped rutile grains. It differs significantly from that of oxidised, uncoated Ti-6Al-4V, which is occupied by a thin α-alumina layer atop rutile. This interface does not change with an additional 72 hours of heat-treatment.

Keywords: High Temperature Oxidation; Decomposition Reaction; Titanium alloy; Ceramic Platelets; Metal Forming

1 Introduction

As a consequence of a unique array of properties, hexagonal boron nitride (h-BN) has a proliferation of applications that span from cosmetics to nanotubes. [1, 2] Due to excellent lubricity, stability at elevated temperatures and high thermal conductivity, prominent amongst these uses are high temperature lubricant and release agent coatings within the metal forming sector. [3, 4] It is therefore vital to know and understand the chemical reactions that h-BN coated metals undergo under industrially relevant conditions.

The hot forming and superplastic forming (SPF) of titanium alloys at around 900°C are widely employed techniques for manufacturing complex titanium sheet structures; predominantly in the aerospace industry but also in fields as diverse as sports equipment and cookware. [5, 6] With these alloys and h-BN both prone to appreciable oxidation at these temperatures, these processes tend to be performed under inert atmospheres. However, the specifics of a particular process may mean that this is not possible. In these cases, the metal forming operation is performed against ambient atmosphere and oxidation becomes a factor.

h-BN coatings are often applied to the pre-formed component and the tool. Tool materials are typically chromia-former alloys, and the 900°C ambient atmosphere fate of h-BN coatings on

examples of these substrates was reported previously by the same author. [7] In this complementary body of work, the chemical reactions undergone by an h-BN coating on the archetypal SPF titanium alloy, Ti-6Al-4V, under these process conditions are elucidated.

Several investigations into the high temperature oxidation of a mass of h-BN powder have been reported in the literature. [8-15] Oxidation has been found to commence at 800°C, [8-11] and proceeds predominantly around the basal plane peripheries of the roundish plate-like particles. The primary reaction is accepted to be Equation 1:

$$BN(s) + \frac{3}{4}O_2(g) \rightarrow \frac{1}{2}B_2O_3(l) + \frac{1}{2}N_2(g) \quad (1)$$

The reaction rate tends to a plateau with extended exposure and it was described by Coles et al. [8] and Hou et al. [13, 15] that this is a consequence of the molten boron trioxide layers around individual particles fusing as they expand and come into contact. This causes the initially discrete entities to agglomerate into a compact bulk that impedes further oxygen from reaching reaction sites. This effect was evident in the thermogravimetric analysis of h-BN powder that was described in the companion piece to this present study. [7] In the first 24 hours at 900°C in dry air, 43.77% of the starting material reacted; in the next 48 hours only a further 7.95% reacted. When h-BN coated chromia-former alloys were exposed to this same temperature and ambient atmosphere, microscale observations revealed particles progressively merging until discrete entities were no longer discernible. It was concluded that in this state, the overlayer was a dispersion of remnant h-BN throughout a boron trioxide matrix, and therefore akin to what is effectively the final stage of reaction for a mass of h-BN powder.

In contrast to an isolated mass of powder, however, when h-BN was in the form of a coating on a chromia-former alloy, this was not the effective final stage of reaction and the oxidation rate did not tend to a plateau. It was found that chromium (III) ions from the concurrently oxidising substrate reacted with boron trioxide in the overlayer to form chromium borate. It was propounded that this served to diminish the diffusion barrier and, ultimately, both the h-BN and its oxide underwent complete decomposition. For a 29 µm thick coating on austenitic stainless steel type 304 (SS304), this occurred after 60 hours.

Despite a number of studies having been published on the high temperature air oxidation mechanisms and kinetics of Ti-6Al-4V, [16-21] documented research concerning the morphology and composition of Ti-6Al-4V scale formed at temperatures higher than 850°C is scant. [22] This is perhaps surprising given that SPF of this alloy has been a key aerospace manufacturing process since the early 1980s. For this reason, the Results section commences with a characterisation of the oxidation of Ti-6Al-4V at 900°C. The aim of this approach is to furnish the reader with an understanding of the surface reactions undergone by the uncoated substrate under the experimental conditions, in order to facilitate comprehension of the results from the coated substrate. Correspondingly, in addition to elucidating the 900°C ambient atmosphere fate of h-BN coatings on Ti-6Al-4V substrates, this research also enabled further insight into the oxidation of the most commonly used titanium alloy. [23]

2 Materials and Methods

2.1 Materials

The same h-BN coating (HeBoCoat 20W, Henze Boron Nitride Products, AG Lauben, Germany) was used as for the experiments on chromia-former substrates. The h-BN powder in this evaporative water-based suspension has a nominal particle size distribution of

D_{10}=0.50 µm, D_{50}=4.90 µm, D_{90}=13.39 µm and D_{100}=27.00 µm, as stated by the manufacturer. This formulation incorporates a combustible organic binder system. From non-isothermal thermogravimetric analysis (TGA) and differential scanning calorimetry (DSC) (Netzsch STA 449 F1 Jupiter) under an 80% nitrogen: 20% oxygen atmosphere (flow rate= 50 ml min^{-1}) and at a heating rate of 5 K min^{-1}, binder combustion was found to commence at 200°C and to be complete by 600°C. Hence, at the temperature of interest, the coating consisted purely of h-BN grains held together by weak cohesive forces. This enabled the interactions between h-BN, the substrate and oxygen only to be characterised.

Ti-6Al-4V coupons (50 x 50 x 5 mm) were donated by Rolls-Royce and the nominal composition of this titanium alloy is detailed in Table 1.

2.2 Coating Application and Heat-treatments

Coatings of reproducible thickness were applied to coupons using an automated spray system (Fanuc M-710iC industrial robot fitted with a Graco AirPro spray gun and linked to a Graco Pro Control 1KS Fluid Management System). Three thin coats were applied to each coupon and each coat was air dried for one hour before application of the next. The dry coating thicknesses were measured using an Elcometer 456.

Coated coupons and uncoated coupons were heat-treated at 900°C in a Pyrotherm (Leicestershire, UK) laboratory furnace, with the thermocouples calibrated to ASTM E220-13 using a Martel PTC8001 precision temperature calibrator. Exposure was followed by an air quench. A minimum of three samples were heat-treated for each exposure time that was investigated.

Oxidation rates of Ti-6Al-4V, SS304 and h-BN coated Ti-6Al-4V at 900°C were each assessed over a 72-hour isothermal period via TGA, using a 10 x 10 x 5 mm sample held in

an alumina beaker. The entire temperature ramp to 900°C for the uncoated samples was performed in a high purity nitrogen atmosphere. The temperature ramp for the coated sample was conducted up to 620°C in an 80% nitrogen: 20% oxygen mixture and thereafter continued to 900°C in nitrogen. This was to ensure that the binders had completely volatilised without h-BN oxidation having commenced when the reaction conditions were reached. For all runs, upon reaching 900°C, the atmosphere was switched to 80% nitrogen: 20% oxygen for the isothermal stage. In the case of the h-BN coated Ti-6Al-4V sample, it was not possible to apply the coating using the automated spray system so the coating was applied manually using a DeVilbiss Advance HD gravity feed spray gun. The same procedure was followed, and the occurrence of TGA events after similar exposure times as, what were reasoned to be, corresponding phenomena in the furnace-based coupon tests, suggests that the coatings applied by the two different means were of similar thickness.

2.3 Surface Analysis

Crystalline phase identification was achieved by x-ray diffraction (XRD) using a Bruker D8 Advance system with Cu Kα radiation, in conjunction with the International Centre for Diffraction Data (ICDD) PDF-2 2009 database. OriginPro 2015 was used to fit diffractogram peaks with a Gaussian-Lorentzian cross product function for the purposes of deconvolution and intensity calculations.

An FEI Quanta 250 field-emission gun scanning electron microscope (SEM) equipped with Oxford Instruments energy and wavelength dispersive spectroscopic electron probe microanalysis (EPMA) capabilities was used to observe surface morphologies and to determine the chemical compositions of absorbed entities and the underlying scale. Due to h-BN and its oxide being electrically non-conductive, samples were gold coated prior to analysis where necessary.

3 Results

3.1 Oxidation of the Ti-6Al-4V Substrate at 900°C

From the TGA plot shown in Figure 1, it can be seen that Ti-6Al-4V oxidises at a considerably faster rate at 900°C than the SS304 substrate that was studied previously. [7] This susceptibility to oxidation is due to (i) the activity of aluminium being too low for a continuous, protective layer of alumina to form at the substrate-oxide interface, [17] and (ii) rutile being porous and having a tendency towards strong lattice disorder. [24, 25] It should be noted that the oxygen uptake does not all contribute to scale formation, for this alloy, as with titanium, is prone to internal oxidation. [20, 26, 27]

The oxide-atmosphere interface of Ti-6Al-4V coupons that were furnace heat-treated for various durations between 10 minutes and 48 hours was consistently a uniform medium brown colour (Figure 2(a)).

Consistent with the overwhelming majority of Ti-6Al-4V oxidation studies, XRD of scale that formed at 900°C generated rutile and α-alumina peaks only (Figure 3). [17-19] That no oxides of vanadium were detected was in spite of up to 2 at.% vanadium being measured throughout the scale cross sections via EPMA. Du et al. [17] attributed this absence to the low concentration that any such phase would be present in, whilst Frangini et al. [19] reasoned that it was a consequence of vanadium dioxide being dissolved in the rutile phase. In contrast, Dong et al. [22] reported XRD evidence for titanium vanadate ($TiVO_4$) in scale formed at 850°C to 1100°C. As up to 2 at.% aluminium was also measured throughout the titanium rich regions, it is suggested here that it may be more accurate to describe the rutile as being a rutile-based solid solution in which are dissolved some vanadium ions and aluminium ions. Such a solution is analogous to that which forms when titanium- and aluminium-based MAX

phase materials undergo high temperature oxidation. [28] This notwithstanding, to avoid potential confusion, this phase is hereafter referred to simply as rutile.

By 10 minutes, both rutile and α-alumina had formed. Due to the analysis depth having been greater than the scale thickness, substrate peaks are also present in the corresponding Figure 3 diffractogram. These had shifted by varying extents to lower 2 Theta values compared to the non-heat-treated sample; a consequence of internal oxidation having increased interplanar distances. The substrate was not detectable through the oxide layer in the 3-hour plot and this diffractogram is essentially superimposable with those from the longer exposure times. This indicates that no further phase changes occurred within the analysis region. The scale had a mean thickness of 39 µm after 3 hours and 152 µm after 24 hours.

The relative intensities of the rutile peaks were significantly different from those of the ICDD powder diffraction file. The diffractograms from this system were dominated by the (101) peak; however, the strongest reference file peak is (110), with (101) being 56% of this intensity. A further notable difference is that the reference file intensity of the (002) peak is 14% that of (110), but in this system it was the stronger of the two. This indicates that rutile formed with preferred orientation, and is supported by the relative peak intensities in diffractograms obtained from powdered scale being equivalent to those in the ICDD file.

At the oxide-atmosphere interface, α-alumina nucleated and grew laterally to cover a rutile base (Figure 4(a)). [17] In previous studies, the α-alumina crystallites have been described as nodular, [17] flower-like, [18] or polyhedral; [22] however, in this study they displayed a tetragonal-like morphology and grew to a maximum length of 1-2 µm. The rutile crystallites were larger and more equiaxed. By 3 hours, an apparently single crystallite thick α-alumina outer-layer was complete, such that no underlying rutile grains could be discerned (Figure 4(b) and (c)). No changes were evident at the outer-interface after longer duration heat-treatments.

In a similar manner to lower temperature oxidation studies, an initial duplex scale structure progressed to a striated structure of alternating thick rutile layers and thin α-alumina layers.[17] The banded structure was pronounced by 3 hours, and the number of layers increased with longer exposure (Figure 4(d) and (e)). The layer at the substrate-oxide interface was always rutile and that at the oxide-atmosphere interface was always α-alumina. This was rationalised by Du et al. who postulated a theory based on simultaneous growth by inward anion and outward cation diffusion, and the preferential reaction of oxygen with titanium at the alloy-oxide interface. [17]

The oxide layer was well adhered to the substrate for up to 40 minutes of 900°C heat-treatment and thereafter it spalled readily. This enabled the inner interface to be analysed. For all durations, it comprised monodisperse domains of <0.5 µm crystallites (Figure 4(f)). Elemental compositions were invariant across the surface: 30±2 at.% titanium, < 1 at.% vanadium, <1 at.% aluminium, balance= oxygen. As such, it is thought that the different crystallite sizes represented grains at different stages of growth.

3.2 Oxidation of h-BN coated Ti-6Al-4V at 900°C

3.2.1 Ambient atmosphere furnace tests

Characterisation of pre-heat-treatment coatings

As can be expected, given that both the h-BN formulation and the application procedure were the same as used for the previous work on chromia-former substrates, the coatings were equivalent.

The mean thickness of the dry coatings was 29.0 ± 2.8 µm and atmosphere interface x-ray diffractograms showed peaks from h-BN and the alloy substrate only (Figure 5(a)). The h-BN particles exhibited the typical planar structure, with smooth surfaces and curved edges. [2]

Subsequent to binder volatilisation, the coating comprised regions of haphazardly stacked, flatly oriented crystallites and agglomerations of variously oriented, smaller crystallites (Figure 5(b)). The latter were possibly due to insufficient homogenisation prior to application. Whilst pores of the order of 1 μm were widespread, instances in which they penetrated the full thickness of the coating were negligible.

Visual Developments

The white, solid-state h-BN coating became translucent and molten with extended exposure. With longer heat-treatment durations, the overlayer thinned until it could no longer be discerned. At this point, the oxide-atmosphere interface could be seen to exhibit a mottled grey and dark brown colouration (Figure 2(b) and (c)). Thereafter, the substrate appearance was invariant following all longer durations of exposure.

XRD Analysis

To commence this section, it should be made clear that the relationship between the concentration of a species and its XRD peak intensities is not linear due to the dependency on the mass absorption coefficient of the sample, which varies with the identity and concentration of all other phases present i.e. matrix effects. Intensities will also be affected by particle reorientations, should these occur. This notwithstanding, it is believed that it is reasonable to make qualitative inferences from the intensity developments that are described.

The trends that were observed for h-BN and boron trioxide on the chromia-former alloys were also seen on Ti-6Al-4V. There was a progressive reduction in intensity of the h-BN peaks and at no point did the rate tend to a plateau (Figure 6). The breadth of the dominant h-BN (002) peak (2θ=26.74°) was essentially constant for the first few exposure times and then it underwent a pronounced narrowing after 7.5 hours. As before, this was possibly due to a

reduction of stacking faults or a relieving of microstrains over the course of the heat-treatments, and this effect dominated the peak broadening that can be expected from decreasing particle size. Boron trioxide features were generated after the shortest exposure time (30 minutes) and there was a trend of increasing intensity up to 24 hours, after which the trend was one of attenuation. For a 29 μm thick coating, neither the h-BN peaks nor the boron trioxide features were present after 48 hours of exposure. After 48 hours, XRD at the atmosphere interface generated rutile and aluminium borate ($Al_4B_2O_9$) peaks only (Figure 7).

While the coating peaks reduced in intensity, rutile and aluminium borate peaks emerged and grew. Both species had formed after 30 minutes of exposure. The rutile peaks progressively grew in intensity up to 12 hours of heat-treatment, and thereafter remained reasonably consistent. This coincided with the substrate peaks no longer being detectable within the analysis depth. As with oxidised uncoated Ti-6Al-4V, the diffractograms were dominated by rutile peaks; however, the ratio of rutile peak intensities was significantly different (Figure 3 and Figure 7(a)). In these systems, the intensity ratios closely resembled those in the ICDD powder diffraction file, thereby indicating no texturing.

The aluminium borate peaks progressively grew throughout the heat-treatments until such time that no coating remained (Figure 8). The relative intensities of the aluminium borate peaks were markedly different from those of the ICDD powder diffraction file. The strongest peak in the reference file is (603); however, in this system (603) was very small and the two most intense peaks were (023) and (520). In the reference file, these two peaks have intensities of 66% and 43%, respectively, of that of (603). These disparities indicate that the aluminium borate formed with a distinct preferred orientation.

Whereas α-alumina was detected in uncoated samples that were heat-treated for as little as 10 minutes, this species did not form at the atmosphere interface of any coated samples (Figure

8). This was the case with exposure times of up to 120 hours having been investigated; that is, up to 72 hours subsequent to complete loss of the coating.

SEM and EPMA Analysis

The reader is reminded that boron trioxide is molten at 900°C and that these SEM-based observations followed an air quench to room temperature. It is the hope that rapid surface cooling created sufficiently faithful snapshots of the system under reaction conditions to enable inferences to be made about the phenomena that occurred.

With increasing exposure time, the morphological changes at the atmosphere interface initially proceeded similarly to those of heat-treated h-BN on chromia-former alloys (Figure 9(a)-(d)). The round plate-like h-BN grains developed into larger planar triangular and hexagonal entities, which subsequently merged into a continuous layer. In the cooled state, this film was peppered with small fissures. The systems thereafter differed. On Ti-6Al-4V, elongated entities with quasi-circular cross sections, as opposed to plate-like species, were observed to have been impressing upon the thinning coating from below (Figure 9(e)). In some cases, these crystallites appeared to have penetrated through the coating. As can also be seen in the Figure 9(e) micrograph, at this point in the heat-treatment large cracks were widespread across the quenched overlayer. These were almost certainly a consequence of differential magnitudes of thermal contraction of boron trioxide and the underlying alloy oxide layer.

In agreement with the XRD results, no remnants of a coating could be seen after 48 hours. It was clear from the microscale morphology and composition of this sample that the coating decomposition reactions had significantly disrupted the alloy oxidation mechanisms. This is

consistent with the macroscale observations regarding the differently coloured atmosphere interface of the uncoated and post-coating oxide layers.

The post-coating atmosphere interface comprised seemingly equiaxed titanium-rich grains with elongated aluminium-rich crystallites protruding through at the grain boundaries (Figure 10). These variously exhibited hollow columnar or solid columnar forms.

The titanium-rich entities comprised 30.0±2.3 at.% titanium, <1 at.% vanadium, <1 at.% aluminium, 4.1±0.9 at.% nitrogen, balance= oxygen. From the XRD results we know that these were rutile-based. EPMA in the vicinity of the aluminium-rich entities detected 21.2±2.4 at.% aluminium, 8.8±1.1 at.% boron, <1 at.% vanadium, <1 at.% titanium, balance= oxygen, which agrees with the assignment of XRD peaks to $Al_4B_2O_9$. The identification of this material as aluminium borate is further supported by the observed morphologies, for one of the reasons behind contemporary interest in synthesising aluminium borate is the microtube [29, 30] and nanorod [31, 32] structures it exhibits. No aluminium-rich entities were observed atop of rutile grains. There were no discernible differences in the morphology or composition of the atmosphere interface of samples that were heat-treated for up to an additional 72 hours.

For samples treated for 18 hours and longer, the scale readily delaminated, which enabled the inner-interfaces and cross sections to also be analysed. The morphology of the inner-interface was unaffected by the presence of a coating. At all heat-treatment durations for which it could be examined, it was equivalent to that of uncoated Ti-6Al-4V scale in that it comprised monodisperse domains of <0.5 µm crystallites. Also akin to the uncoated samples, elemental compositions were invariant across the surface: 30.4±2.0 at.% titanium, <1 at.% vanadium, <1 at.% aluminium, 3.4±0.3 at.% nitrogen, balance=oxygen.

The cross sections up until 48 hours of exposure time possessed a duplex structure (Figure 11(a)-(c)). The upper region was composed of rutile interspersed by the aluminium borate crystallites, oriented almost perpendicular to the surface plane. This is in the agreement with the distinct texturing indicated by the aluminum borate XRD data. Underlying this, the rutile solid solution contained <2 at.% aluminum, <2 at.% vanadium and 3-5 at.% nitrogen as solutes. Grain sizes decreased towards the alloy interface, indicative of those in the lower regions being at an earlier stage of growth. In support of other data presented here, the coating can clearly be seen atop of the 18-hours cross section but is not present in the 48-hours micrograph.

The presence of both titanium- and aluminium-based species at the atmosphere interface and only solute containing rutile at the substrate interface is consistent with previous work concerning the oxidation of uncoated Ti-6Al-4V. [17] As such, this indicates that the oxide layer that grew in the coated system also grew via both simultaneous outward diffusion of titanium (IV) ions and aluminium (III) ions, and inward diffusion of oxygen anions that reacted with titanium at the alloy surface. As aluminium borate was detected in the shortest exposure time diffractograms, the base of the columnar crystallites can be used as a demarcation line to separate the inward and outward growth regions. This can then be used to determine which was dominant. At 18 h, the aluminum borate crystallites had a mean length of 11 μm and the oxide layer had a total thickness of approximately 36 μm; at 48 h, these were measured to be 17 μm and 68 μm. From this, it is evident that oxide layer growth occurred predominantly at the inner interface.

After 60 hours, the thickness of the oxide layer was in the region of 105 μm (Figure 11d). This approximately 50% increase between 48 hours and 60 hours indicates that there was a post-coating acceleration in the rate of scale growth. The length of the aluminium borate

crystallites after 60 hours were equivalent to those at 48 hours. From this exposure time onwards, horizontal, thin aluminium-rich bands were commonplace in the lower region of the oxide layer. This striated structure was equivalent to that of the scale which formed on uncoated Ti-6Al-4V that was heat-treated at 900°C for 3 hours or longer.

3.2.2 Thermogravimetric Analysis

A Ti-6Al-4V cuboid that had h-BN applied to all faces was exposed to a 900°C isothermal TGA programme for 72 hours under 80% nitrogen: 20% oxygen. The resultant trace is shown in Figure 12, along with that from the early stages of exposure of equivalently heat-treated uncoated Ti-6Al-4V (the reader is referred to Figure 1 for the full version of this trace). The inset to Figure 12 shows the initial mass gain undergone by the coated Ti-6Al-4V system alongside the full plot from isolated coating exposed to the same conditions, which was described previously. [7]

All three systems underwent mass increases only, and at rates that progressively decreased from comparatively fast initial values. The early stage rate for h-BN coated Ti-6Al-4V was lower than that for uncoated Ti-6Al-4V and considerably greater than that for the isolated coating. This can be understood by considering that at this point in the heat-treatment, the coating comprised discrete entities and so oxygen could impinge directly upon the substrate via intergranular gaps. Consequently, there will have been a significant contribution from oxidation of both the coating and the substrate. It should be noted that there will also have been a contribution from direct substrate oxidation at the sample edges and vertices. This was due to it not being possible to apply coating at these points without compromising a uniform coverage on the faces.

As with isolated h-BN, the gradually decreasing rate of mass gain for h-BN coated Ti-6Al-4V proceeded to drop-off with a pronounced curvature. This feature is therefore similarly

attributed to the molten boron trioxide around individual h-BN grains merging into a continuum. However, the curvature was more gentle and at no point thereafter did the rate tend to a plateau. Both of these effects are thought to be consequences of the oxygen permeability of the overlayer, and the continued oxidation of the substrate and decomposition of the coating that resulted from this. This notwithstanding, at all times the rate of mass increase was less than that of uncoated Ti-6Al-4V, which reflects the oxygen barrier/getter functionality of the overlayer.

A development unique to the h-BN coated Ti-6Al-4V system can be seen to have commenced after approximately 51 hours of exposure. The rate of mass gain increased abruptly here, and it is reasoned that this marked the point of complete coating decomposition. Thereafter, the plot exhibited an almost linear form until the end of the heat-treatment. This sustained period of enhanced mass gain supports the conclusion from the coupon cross section SEM and EPMA analysis that the substrate oxide layer experienced accelerated growth upon complete coating decomposition. It may be inferred from this having occurred after a slightly longer exposure time than with the furnace-based experiments, that the coating that was applied for the TGA experiment was slightly thicker.

It is worth briefly considering the effects that altering the coating thickness can be expected to have on Δm. A thicker coating than that applied here would provide greater protection to the substrate. As such, it is expected that the rate of mass gain at each stage prior to complete decomposition would be lower. Furthermore, with a greater amount of coating to undergo reaction, a longer exposure time would be required for complete decomposition to occur. Hence, the point at which the rate of mass gain increases would be delayed. The opposite would clearly be the case with a thinner coating.

4 Discussion

The 900°C ambient atmosphere fate of an h-BN coating on a Ti-6Al-4V substrate was qualitatively similar to that on chromia-former alloys. Unlike with a mass of h-BN powder, the oxidation rate did not tend to a plateau and both h-BN and its oxide underwent complete decomposition. As previously, to understand why, consideration must be given to the products of the reactions between the alloy elements and the coating.

From the shortest duration of exposure, aluminium borate ($Al_4B_2O_9$) was detected in diffractograms taken at the atmosphere interface. This indicates that a reaction readily took place between the boron trioxide that formed around the basal planes of the oxidising h-BN particles and an aluminium-based species that had its origins in the substrate. Despite titanium being the dominant Ti-6Al-4V component, there were no titanium borate peaks in the XRD plots from this system and nor was any boron detected in the oxide layer rutile grains.

$Al_4B_2O_9$ is one of two aluminium borate species that are stable in ambient atmosphere, with the other being $Al_{18}B_4O_{33}$. [33] $Al_4B_2O_9$ can form at temperatures as low as 780°C, whilst temperatures greater than 1000°C are required for $Al_{18}B_4O_{33}$. [34] This material has been synthesised via various means that include a sol-gel route followed by calcination, [35] chemical vapour deposition, [29] precipitation followed by annealing, [36] ball milling followed by calcination, [37, 38] and direct reactions of mixtures at elevated temperatures in air [31, 32, 34, 39] or an argon atmosphere. [40] Across this range of reaction systems, it is the consensus that the key reaction takes place between alumina and boron trioxide. One popular proposed mechanism by which this occurs is via the solution-liquid-solid (SLS) growth mechanism. [41] According to this theory, alumina or aluminium dissolves in molten boron trioxide and then when the solution becomes supersaturated, aluminium borate crystallites form and are

precipitated out. [32, 38-40] In the case of aluminium, this may follow the thermite-type reduction of boron trioxide by aluminium. [37]

The absence of alumina peaks in diffractograms taken both during and subsequent to the decomposition of h-BN and boron trioxide, however, suggests that an alternative reaction mechanism took place in this system. This is analogous to the case of heat-treated boron trioxide on SS304 where manganese borate but no manganese oxides were detected. [7] Whilst it is possible that the rate of reaction to form the borate species was exceptionally fast compared to the rate of reaction to form the oxide species, it is thought extremely unlikely that the second stage reaction could happen so fast and in such a complete manner as to not leave any XRD detectable trace of the intermediate oxide. Indeed, a driving force behind the development of new aluminium borate synthesis methods has been to increase the purity of the products as it is usually the case that they contain oxide impurities. [35] Hence, that no such impurities were detected in the aluminium borate formed in this study also supports an alternative reaction mechanism.

A third reason why it is thought that the reaction between boron trioxide and the concurrently oxidising Ti-6Al-4V substrate was not between alumina and boron trioxide, is the size and temporal-dependence of size of the aluminium borate crystallites. In all previous studies that have been identified by the author, the product crystallites have grown to a maximum length of around 2 μm and there have been no reports of morphological or structural modifications occurring with extended reaction times, beyond a short threshold duration. [31] In contrast, those that formed in this system increased in length throughout the heat-treatments and they had a final mean length of 17 μm. Furthermore, it can reasonably be expected that they would have continued to grow had the supply of boron trioxide not become exhausted.

It is therefore proposed that as the h-BN and Ti-6Al-4V substrate concurrently oxidised, outwardly diffusing aluminium (III) ions from the alloy reacted with and consumed boron trioxide at the scale-coating interface to form aluminium borate. That no alumina formed indicates that all the aluminium ions that diffused through the oxide layer reacted with boron trioxide. The vertical orientation of the product crystallites at rutile grain boundaries shows that these grain boundary short circuit routes were the preferred cation diffusion paths, which is in line with what can be expected according to both thermodynamic and kinetic considerations. [42]

At this point it is pertinent to comment on the finding from the analogous chromia-former experiments that appreciable manganese and iron were present at the scale-film interface, but no manganese or iron oxides. [7] Based on this, it was proposed that the overlayer inhibited the formation of these oxide species. This was part of the reasoning behind the conclusion that chromium borate had formed via chromium (III) ions reacting with boron trioxide rather than reaction between chromia and boron trioxide. That rutile formed readily in the h-BN coated Ti-6Al-4V system is not inconsistent with this prior line of reasoning. This is because titanium dioxide has a lower Gibbs free energy of formation and hence a significantly lower dissociation pressure than the oxides of manganese, iron and chromium.

Given the equivalencies that have been described between the fate of h-BN on Ti-6Al-4V and that on the chromia-forming substrates at 900°C, the essence of the model that was previously developed to explain the observed phenomena applies equally to this system (Figure 13).

As the h-BN grains oxidised, they became enveloped around their basal plane peripheries by a growing layer of molten boron trioxide that caused the individual entities to expand. This was a consequence of the molar volume of boron trioxide at the reaction temperature being a

factor of four greater than that of h-BN. [43, 44] With subsequent exposure, the grains merged into a continuous dispersion of h-BN through a molten boron trioxide matrix. With the substrate oxidising concurrently, outwardly diffusing aluminium (III) ions reacted with, and consumed, the boron trioxide matrix to form aluminium borate. This depleted the diffusion barrier and maintained the oxidation of h-BN at a higher rate than would be the case in the absence of the reactive substrate. Ultimately, the oxidation of h-BN proceeded to completion and the boron trioxide was consumed in entirety by the underlying scale.

The presence of 3-5 at.% nitrogen in the rutile grains suggests that when this species was liberated following the reaction of oxygen with h-BN, two pathways were open to it. It could depart as a gaseous species, or if the reaction occurred in sufficiently close proximity to surface adsorption sites, it could enter the scale as nitrogen anions. The similarity of the nitrogen ionic radius to that of oxygen, and the essentially uniform concentration of nitrogen throughout the full thickness of the oxide layer suggests that the diffusing nitrogen anions behaved as oxygen anions. This is supported by the absence of XRD peaks corresponding to nitrogen containing species, which indicates that nitrogen was present as a randomly distributed solute in solid solution. That no nitrogen was detected in the aluminium-rich oxide material or in the chromia-former oxide layers was possibly due to an increased affinity of titanium towards nitrogen, relative to aluminium and chromium. [45]

It may seem surprising when considering the significantly greater oxidation rate of Ti-6Al-4V relative to that of SS304, that complete decomposition occurred in 80% of the time. However, it was not the overall substrate oxidation rate that determined the influence of a substrate on the rate of decomposition of h-BN, but the rate at which reactive cations diffused through the oxide layer to the oxide-atmosphere interface. As was determined from the coupon cross section SEM and EPMA analysis, the Ti-6Al-4V scale grew predominantly at

the alloy-oxide interface. Furthermore, whilst outward cation diffusion in the stainless steel systems was almost exclusively in the form of the reactive chromium (III), outward cation diffusion through Ti-6Al-4V scale was dominated by titanium (IV), which did not react with boron trioxide.

The absence of any discernible changes at the post-coating atmosphere interface with further heat-treatment was akin to that of the uncoated Ti-6Al-4V oxide layer not changing subsequent to 3 hours of exposure time. This has also been reported for Ti-6Al-4V oxidised at 750°C for longer than 72 hours, and a theory to explain it was developed by Du et al. [17, 18] It was proposed that when growth stresses (which increase with scale thickness) caused by the mismatch in expansion coefficients between the scale and the substrate reach a critical level, cracks form at the alloy-oxide interface to relieve them. Thereafter, the progression of oxidation mechanisms start anew at these discontinuities, with a consequent cessation of cation diffusion to the atmosphere interface. This results in multi-layered scale in which thin horizontal bands of alumina exist between thicker bands of rutile. It is thought that this theory can also explain the static post-coating atmosphere interface because (i) the cessation of developments at this interface coincided with the scale adopting a multilayer structure, and (ii) the adoption of a multilayer structure coincided with a post-coating acceleration of scale growth. Indeed, by virtue of being able to rationalise findings from the oxidation of h-BN coated Ti-6Al-4V by invoking the prior theory concerning the oxidation of uncoated Ti-6Al-4V, additional support is given to the validity of that theory.

The research that has been described fulfilled the preproject aim of determining the fate of an h-BN coating on the archetypal SPF titanium alloy under 900 °C ambient atmosphere process conditions. In doing so, an interesting reaction system in which a metal and a ceramic undergo concurrent and interrelated high temperature corrosion has been discovered.

Furthermore, the findings indicate that the aluminum borate which formed did so via, what is thought to be, a hitherto unreported mechanism. With there being significant contemporary interest in fabricating aluminum borate as a strengthening agent for composite materials, [46, 47] these findings may provide insight into a pathway by which to synthesise larger and purer aluminium borate crystallites than is possible from conventional routes.

5 Conclusions

1. In air at 900°C, the fate of an h-BN coating on a Ti-6Al-4V substrate was qualitatively similar to that on chromia-former alloys. This is in spite of the two substrate types comprising dissimilar alloying elements.
2. As the h-BN grains became encompassed around their basal planes by molten boron trioxide, outwardly diffusing aluminium (III) ions from the underlying substrate reacted with it to form aluminium borate. This diminished the effectiveness of the protective diffusion barrier. Despite being the dominant cation in Ti-6Al-4V scale, titanium (IV) was not found to react with boron trioxide.
3. Ultimately, both h-BN and its oxide underwent complete decomposition. The post-coating atmosphere interface consisted of elongated aluminium borate crystallites protruding though at the grain boundaries of apparently equiaxed, 3-5 at.% nitrogen-doped rutile grains. 3-5 at.% nitrogen was also dissolved in rutile grains throughout the scale cross section.
4. The post-coating atmosphere interface did not change with further heat-treatment. This was attributed to the oxide layer growth rate having sharply accelerated upon decomposition of the barrier film, which led to discontinuities forming at the alloy-oxide interface to relieve the resultant growth stresses.

Acknowledgements

The author would like to thank Nicola Zuelli and Paul Blackwell for their invaluable support in enabling this study; Duncan Rodger and Jacqueline Schramm for their help when conducting the heat-treatment tests; and Fiona Sillars and Tiziana Marrocco for their assistance at the Advanced Materials Research Laboratory, University of Strathclyde.

6 References

[1] D. Golberg, Y. Bando, Y. Huang, T. Terao, M. Mitome, C. Tang, C. Zhi ACS nano. 2010, 4, 2979-2993.

[2] A. Lipp, K. A. Schwetz, K. Hunold Journal of the European Ceramic Society. 1989, 5, 3-9.

[3] P. A. Friedman, S. G. Luckey in High-temperature lubricants for superplastic forming of metals, Vol. (Ed. G. Giuliano), Elsevier, Cambridge, 2011, pp.72-82.

[4] S. Rudolph Interceram. 1993, 42, 302-305.

[5] K. Osada Journal of materials processing technology. 1997, 68, 241-245.

[6] D. G. Sanders, M. Ramulu Journal of materials engineering and performance. 2004, 13, 744-752.

[7] C. D. Fleming Materials and Corrosion; in press. 2019.

[8] N. G. Coles, D. R. Glasson, Jayaweer.Sa J Appl Chem. 1969, 19, 178-181.

[9] V. A. Lavrenko, A. F. Alexeev Ceram Int. 1986, 12, 25-31.

[10] L. Podobeda, A. Tsapuk, A. Buravov Powder Metallurgy and Metal Ceramics. 1976, 15, 696-698.

[11] M. D. Shieh, C. Lee Chem Eng Sci. 1993, 48, 1851-1857.

[12] N. Jacobson, S. Farmer, A. Moore, H. Sayir J Am Ceram Soc. 1999, 82, 393-398.

[13] X. M. Hou, Z. Y. Yu, Z. Y. Chen, K. C. Chou, B. J. Zhao J Am Ceram Soc. 2013, 96, 1877-1882.

[14] K. Oda, T. Yoshio J Mater Sci. 1993, 28, 6562-6566.

[15] H. Xinmei, L. Yanxiang, Y. Ziyou, C. Kuo‐Chih International Journal of Applied Ceramic Technology. 2015, 12, E138–E145.

[16] V. Barranco, M. L. Escudero, M. C. García-Alonso Acta Biomaterialia. 2011, 7, 2716-2725.

[17] H. L. Du, P. K. Datta, D. B. Lewis, J. S. Burnellgray Corros Sci. 1994, 36, 631-642.

[18] H. L. Du, P. K. Datta, D. B. Lewis, J. S. Burnell-Gray Oxidation of Metals. 1996, 45, 507-527.

[19] S. Frangini, A. Mignone, F. Dericcardis J Mater Sci. 1994, 29, 714-720.

[20] H. Guleryuz, H. Cimenoglu J Alloy Compd. 2009, 472, 241-246.

[21] S. Kumar, T. S. N. S. Narayanan, S. G. S. Raman, S. K. Seshadri Mater Chem Phys. 2010, 119, 337-346.

[22] E. Dong, W. Yu, Q. Cai, L. Cheng, J. Shi Oxidation of Metals. 2017, 88, 719-732.

[23] R. R. Boyer Materials Science and Engineering: A. 1996, 213, 103-114.

[24] P. E. Hovsepian, C. Reinhard, A. Ehiasarian Surface and Coatings Technology. 2006, 201, 4105-4110.

[25] C. Leyens in Oxidation and Protection of Titanium Alloys and Titanium Aluminides, Vol. (Eds.: C. Leyens, M. Peters), Wiley-VCH ; [Chichester : John Wiley] [distributor], Weinheim, 2003, pp.187-230.

[26] D. A. Brice, P. Samimi, I. Ghamarian, Y. Liu, R. M. Brice, R. F. Reidy, J. D. Cotton, M. J. Kaufman, P. C. Collins Corros Sci. 2016, 112, 338-346.

[27] F. Pitt, M. Ramulu Journal of Materials Engineering and Performance. 2004, 13, 727-734.

[28] M. Barsoum, N. Tzenov, A. Procopio, T. El-Raghy, M. Ali Journal of The Electrochemical Society. 2001, 148, C551-C562.

[29] Y. Li, R. P. Chang Mater Chem Phys. 2006, 97, 23-30.

[30] R. Ma, Y. Bando, T. Sato, C. Tang, F. Xu Journal of the American Chemical Society. 2002, 124, 10668-10669.

[31] J. Zhang, J. Lin, H. Song, E. Elssfah, S. Liu, J. Luo, X. Ding, C. Tang, S. Qi Materials Letters. 2006, 60, 3292-3295.

[32] J. Zhou, D. Su, J. Luo, M. Zhong Materials Research Bulletin. 2009, 44, 224-226.

[33] P. J. M. Gielisse, W. R. Foster Nature. 1962, 195, 69-70.

[34] X. Tao, X. Wang, X. Li Nano letters. 2007, 7, 3172-3176.

[35] C. Tang, E. Elssfah, J. Zhang, D. Chen Nanotechnology. 2006, 17, 2362-2367.

[36] A. Douy Solid state sciences. 2005, 7, 117-122.

[37] Y. Birol Mater Chem Phys. 2012, 136, 963-966.

[38] Z. Yu, N. Zhao, E. Liu, C. Shi, X. Du, J. Wang Powder technology. 2011, 212, 310-315.

[39] M. F. Hernández, G. Suárez, M. Cipollone, M. S. Conconi, E. F. Aglietti, N. M. Rendtorff Ceram Int. 2017, 43, 2188-2195.

[40] Y. Liu, Q. Li, S. Fan Chemical physics letters. 2003, 375, 632-635.

[41] K. W. Kolasinski Current Opinion in Solid State and Materials Science. 2006, 10, 182-191.

[42] A. Paul, T. Laurila, V. Vuorinen, S. V. Divinski in Short-Circuit Diffusion, Vol., Springer International Publishing, Cham, 2014, pp.429-491.

[43] Napolitano.A, P. B. Macedo, E. G. Hawkins J Am Ceram Soc. 1965, 48, 613-616.

[44] V. L. Solozhenko, T. Peun Journal of Physics and Chemistry of Solids. 1997, 58, 1321-1323.

[45] J.-P. Bars, D. David, E. Etchessahar, J. Debuigne Metallurgical Transactions A. 1983, 14, 1537-1543.

[46] K. Suganuma, T. Fujita, N. Suzuki, K. Niihara Journal of Materials Science Letters. 1990, 9, 633-635.

[47] M. Zheng, K. Wu, H. Liang, S. Kamado, Y. Kojima Materials Letters. 2002, 57, 558-564.

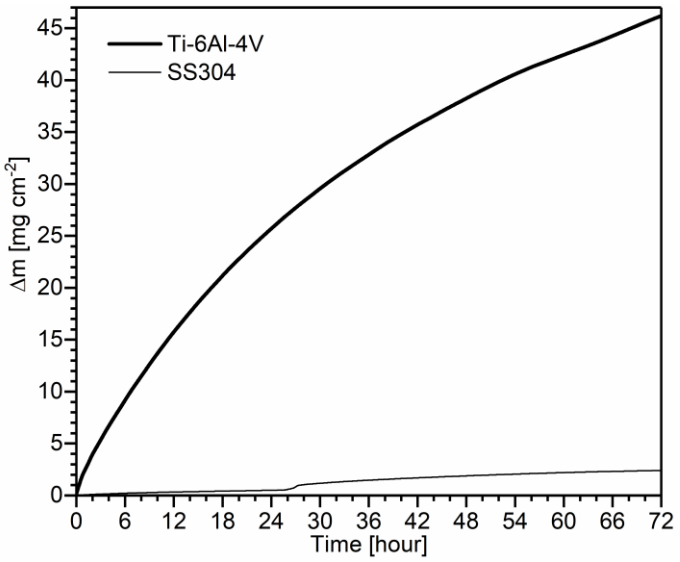

Figure 1. TGA plots from Ti-6Al-4V and SS304 that were exposed to a dry 80% N_2: 20% O_2 atmosphere for 72 hours at 900°C.

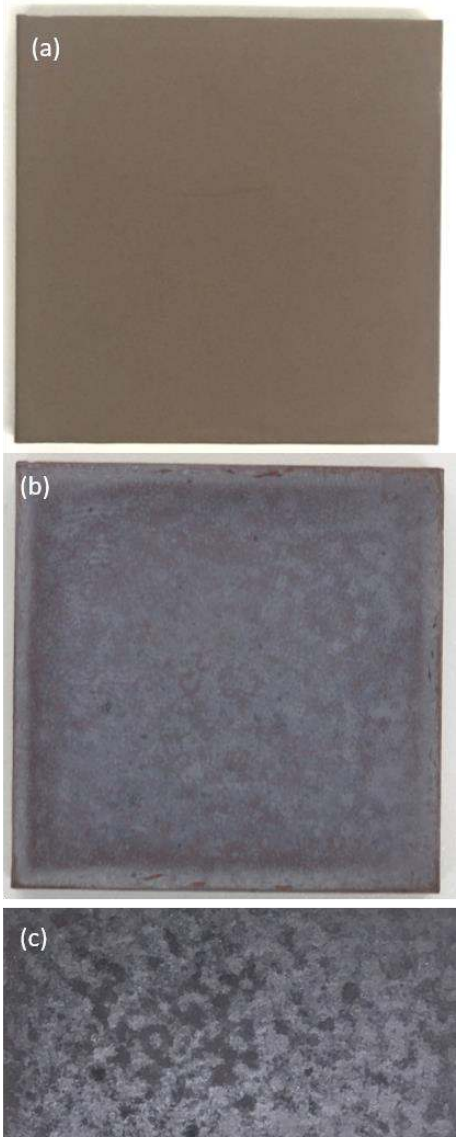

Figure 2. (a) The atmosphere interface of the scale that formed on Ti-6Al-4V coupons that were heat-treated in ambient atmosphere at 900°C was consistently a uniform medium brown colour. That shown was heat-treated for 3 hours. (b) The atmosphere interface of the h-BN coated Ti-6Al-4V coupons subsequent to complete coating decomposition at 900°C in ambient atmosphere was consistently mottled grey and dark brown in colour. (c) Close up of a region of the surface shown in (b) to highlight fine detail. The coupons shown had the dimensions 50 x 50 x 5 mm.

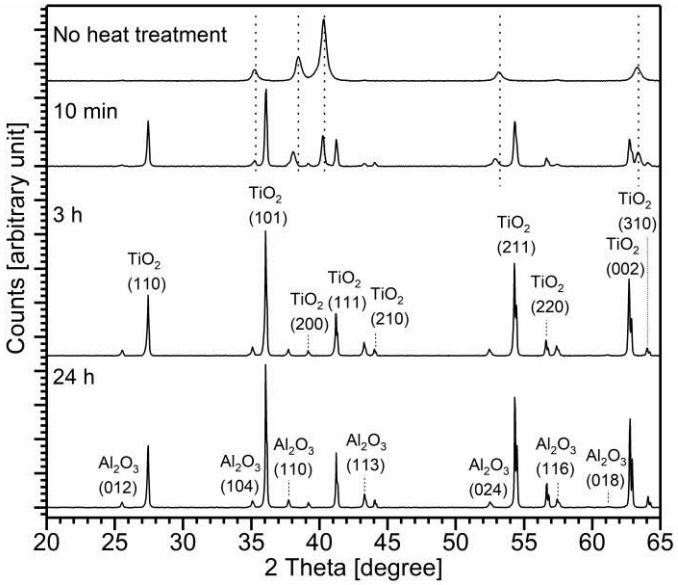

Figure 3. Oxide-atmosphere interface XRD plots showing the development of crystalline species in the oxide layer formed on Ti-6Al-4V that was heat-treated in ambient atmosphere at 900°C. The peaks are indexed according to the ICDD reference files: α-Al2O3 (PDF 01-070-5679), Rutile (PDF 01-086-0148). The dotted lines extending from the upper axis are to aid visualisation of the substrate peak shifts after 10 minutes of exposure.

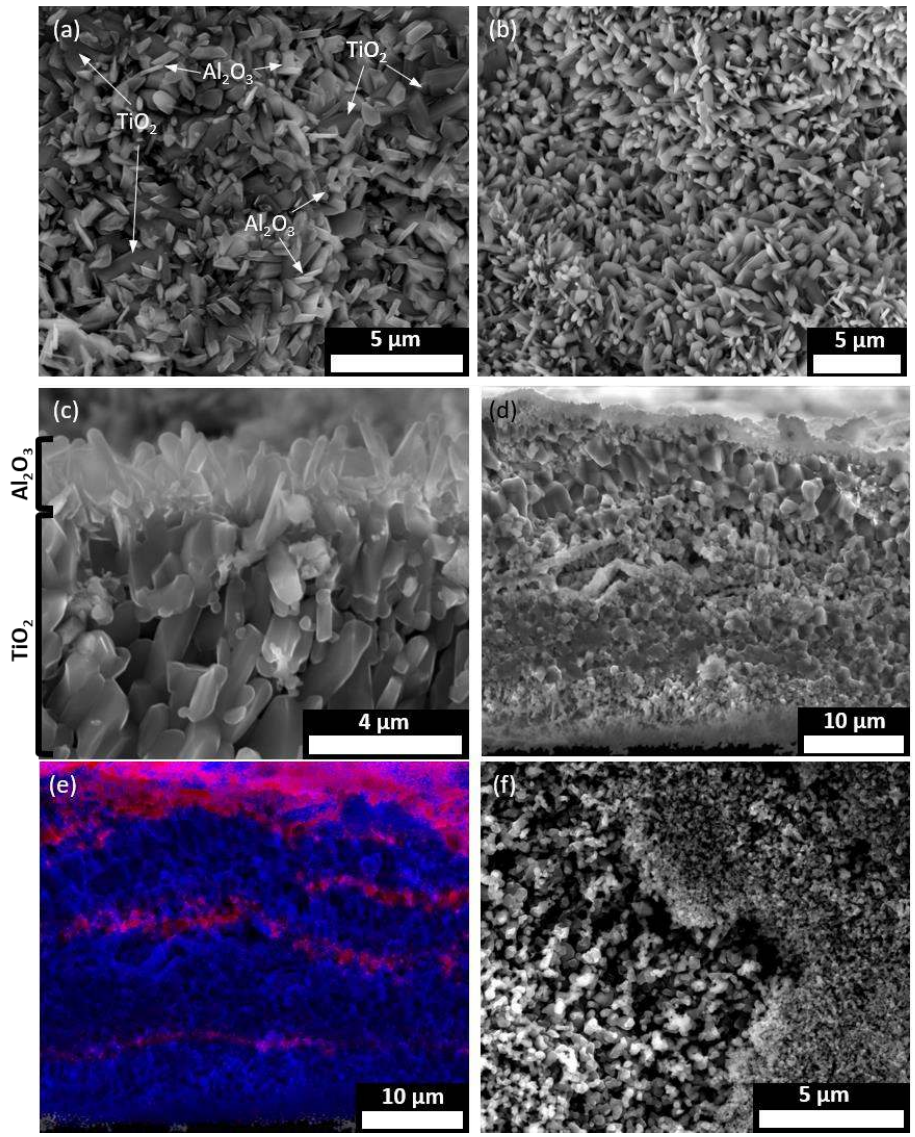

Figure 4. SEM micrographs of the scale that formed on uncoated Ti-6Al-4V during atmospheric exposure at 900°C. (a) Oxide-atmosphere interface after 40 minutes of heat-treatment: regions of incomplete α-Al_2O_3 coverage atop TiO_2 are discernible. To aid clarity, examples of each of the morphologically distinct crystallite types are highlighted. (b) Oxide-atmosphere interface after 3 hours of heat-treatment: complete coverage of α-Al_2O_3 (c) Upper region of scale cross section after 3 hours of heat-treatment (d) Full scale cross section of scale formed after 3 hours of heat-treatment (e) EPMA map of (d); blue= titanium and red= aluminium (f) Inner interface after 3 hours of heat-treatment: two monodisperse domains of differently sized crystallites are observable. Elemental compositions were equivalent for both.

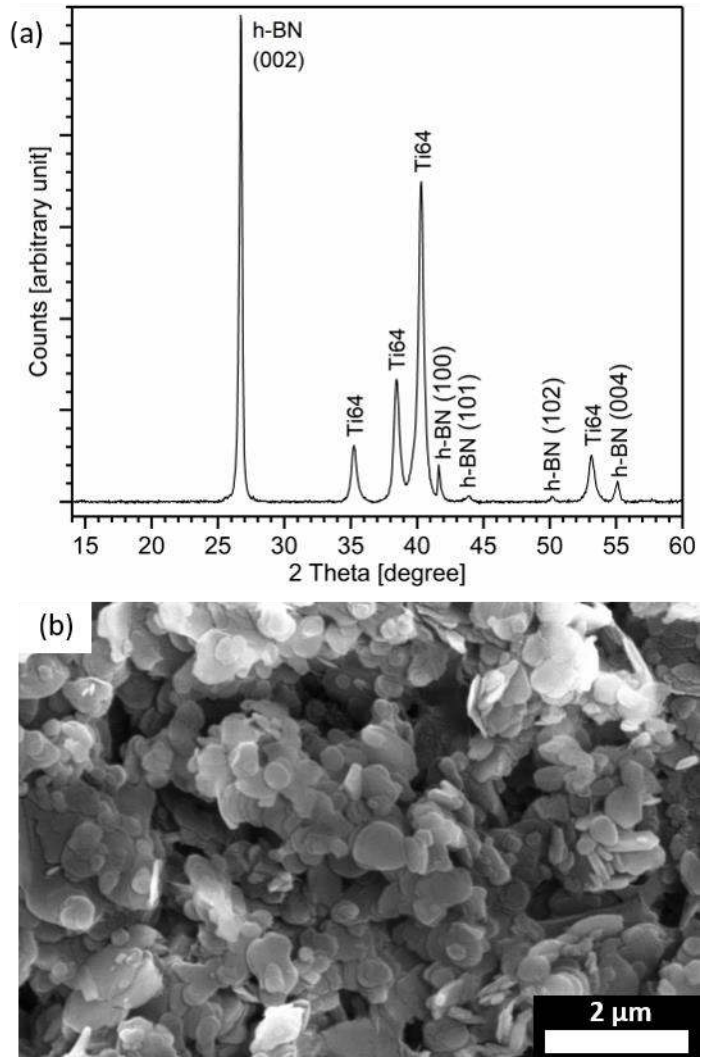

Figure 5. (a) XRD plot that was taken at the atmosphere interface of h-BN coated Ti-6Al-4V prior to heat-treatment. The substrate peaks are labelled and the h-BN peaks are indexed according to the ICDD reference file PDF 00-034-0421. (b) SEM micrograph showing the h-BN coating subsequent to volatilisation of organic binders.

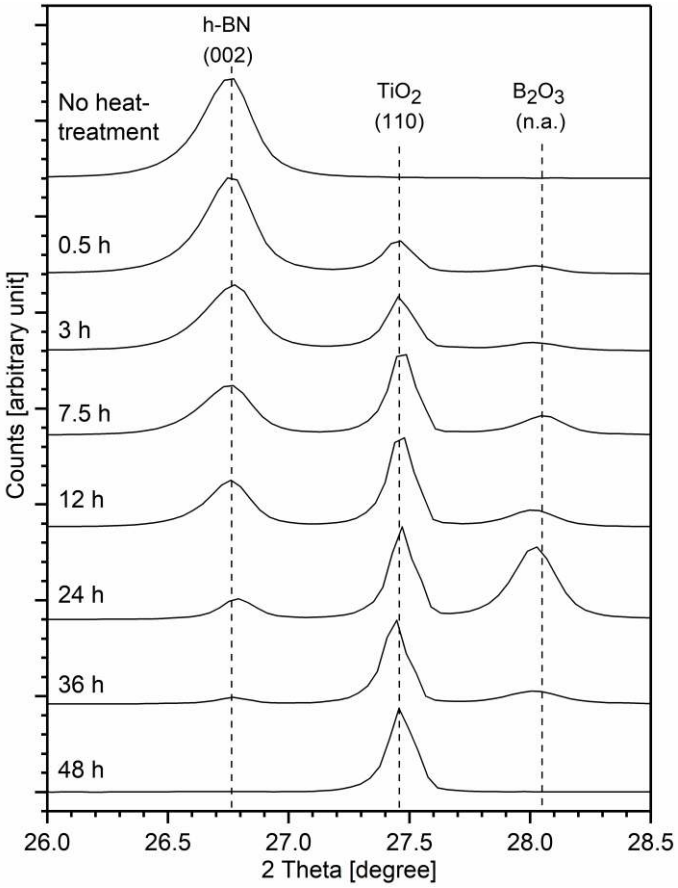

Figure 6. XRD plots that were taken at the atmosphere interface of h-BN coated Ti-6Al-4V coupons that were heat-treated for various durations at 900°C in ambient atmosphere. This 2 Theta range shows the progression of the strongest h-BN (PDF 00-034-0421) and B_2O_3 (PDF 00-013-0570) peaks, alongside that of the rutile (110) peak (PDF 01-086-0148), as exposure time was increased.

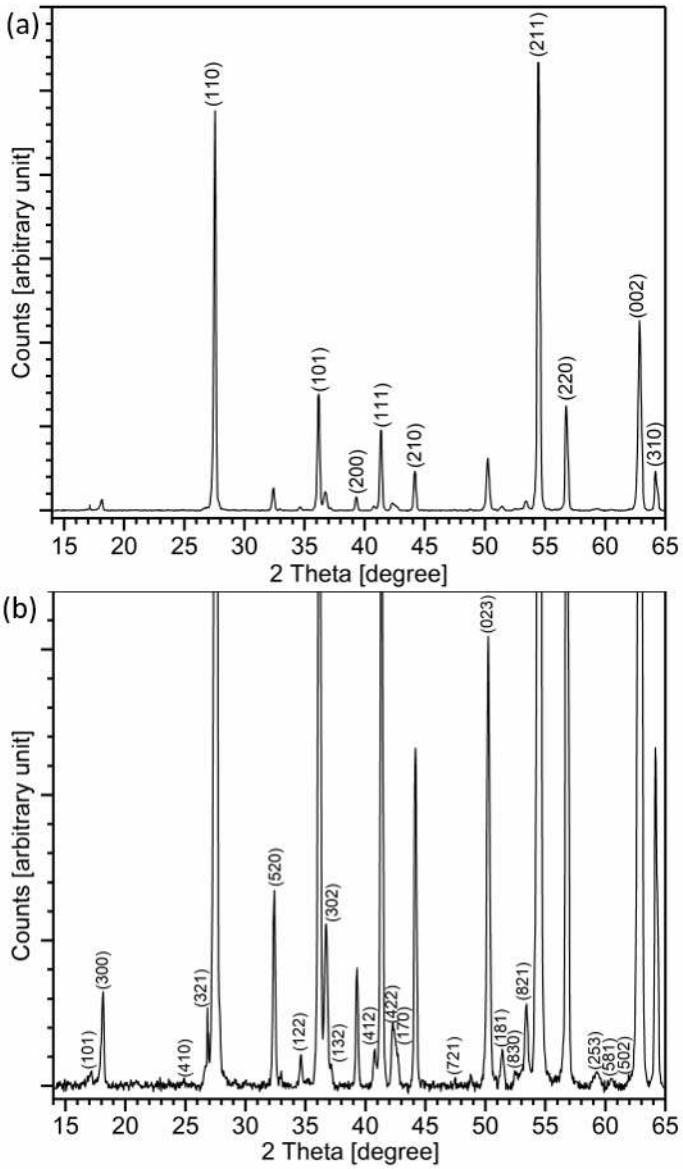

Figure 7. Diffractogram taken at the atmosphere interface of h-BN coated Ti-6Al-4V that was exposed to ambient atmosphere at 900°C for 48 hours. (a) Full ordinate range is shown. Rutile peaks are indexed according to the ICDD reference file (PDF 01-086-0148) (b) The dominant rutile peaks are truncated to aid clarity of the $Al_4B_2O_9$ peaks (PDF 00-009-0158).

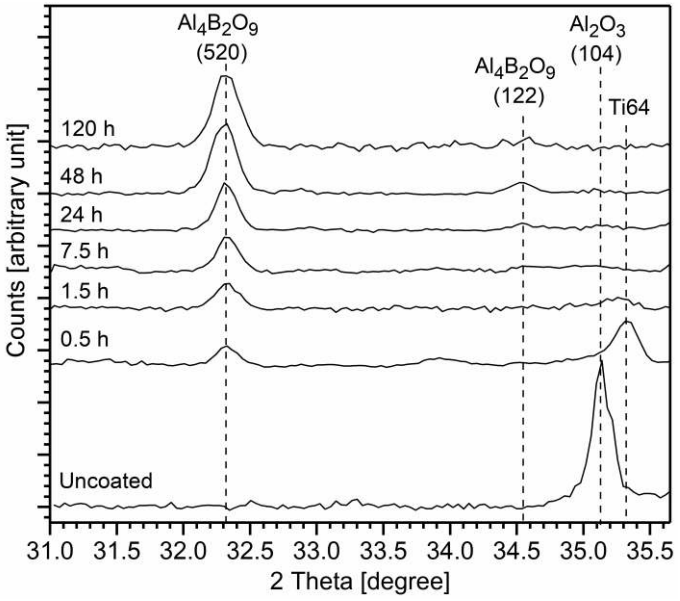

Figure 8. XRD plots that were taken at the atmosphere interface of h-BN coated Ti-6Al-4V coupons that were heat-treated for various durations at 900°C in ambient atmosphere. Also shown is a diffractogram from uncoated Ti-6Al-4V that was exposed to these same conditions for 24 hours. This 2 Theta range shows the development of $Al_4B_2O_9$ (PDF 00-009-0158) as exposure time was increased, and also that Al_2O_3 (PDF 00-075-1862) did not form in the near surface region of any of the heat-treated coated samples.

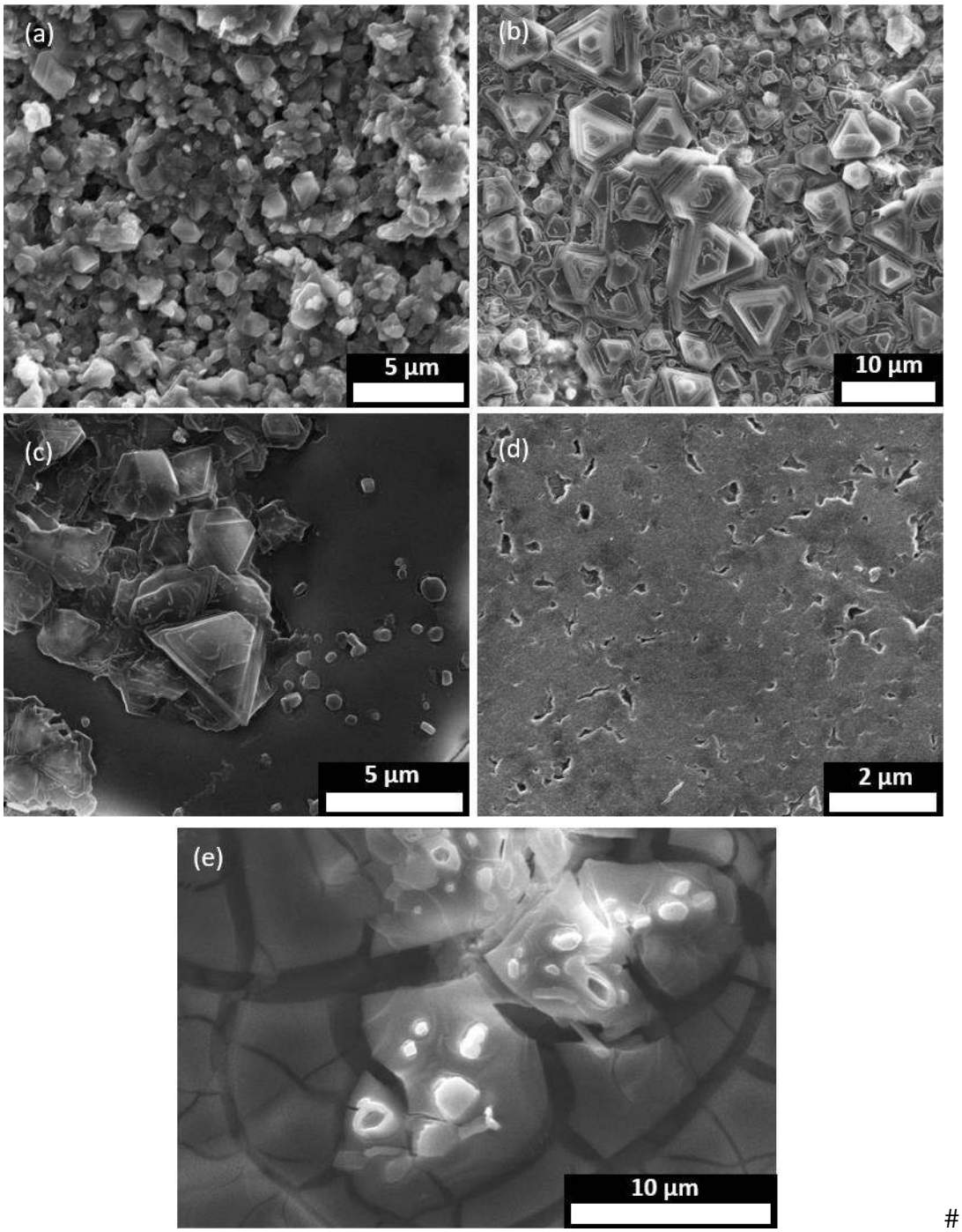

#

Figure 9. SEM micrographs taken at the atmosphere interface when h-BN coated Ti-6Al-4V was exposed to ambient atmosphere at 900°C for (a) 1.5 h (b) 7.5 h (c) 18 h (d) 24 h (e) 36 h, and subsequently air quenched.

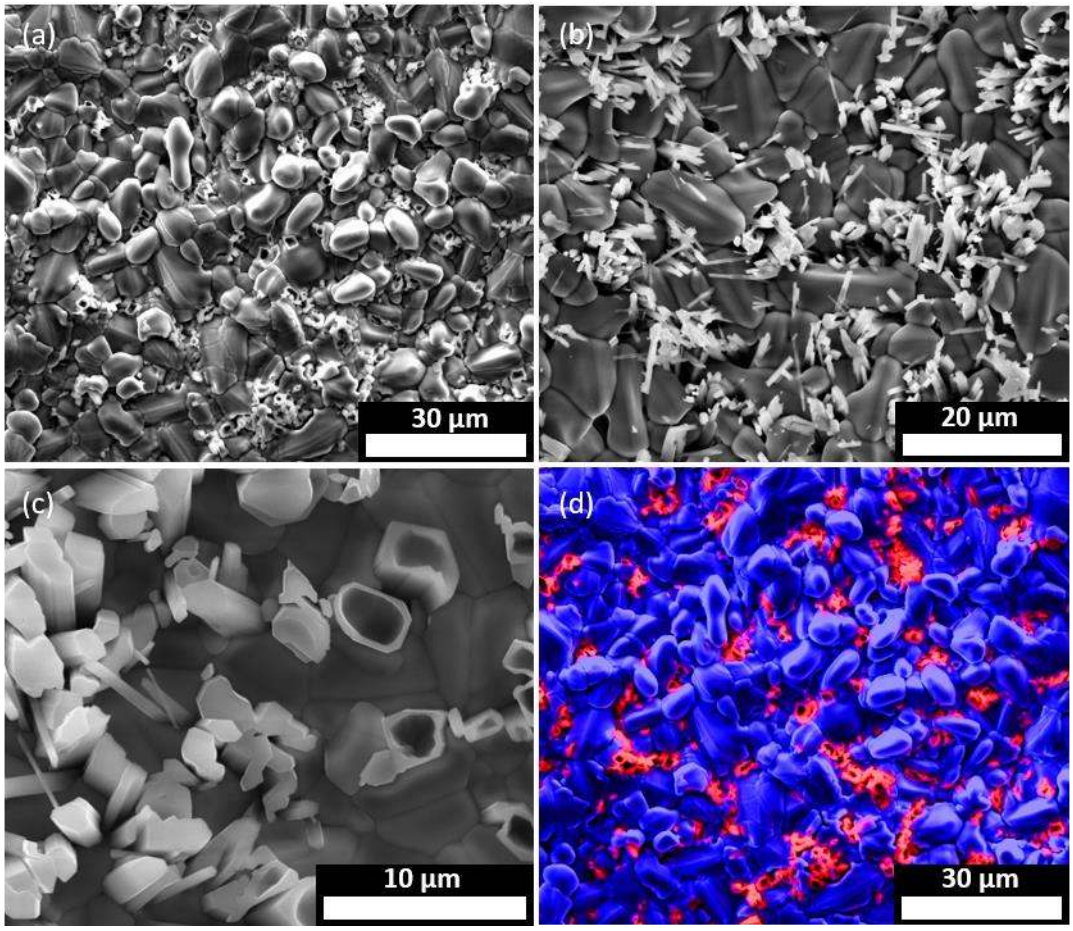

Figure 10. (a) – (c) SEM micrographs of the atmosphere interface of h-BN coated Ti-6Al-4V that was heat-treated in ambient atmosphere at 900°C for 48 hours. Microtube and microrod aluminium borate crystallites can be seen protruding through at the boundaries between more-equiaxed rutile crystallites. (d) EPMA map of (a); blue= titanium and red= aluminium.

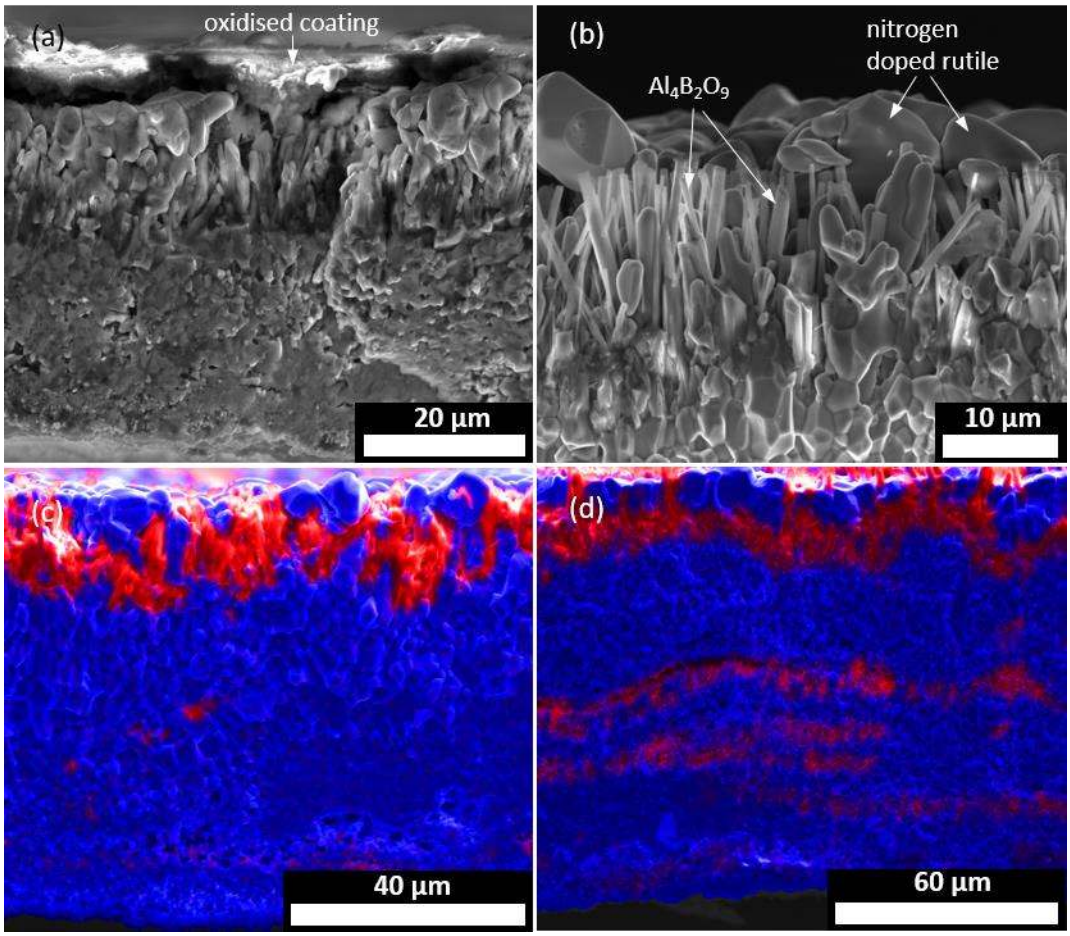

Figure 11. SEM micrographs and EPMA maps of the coated Ti-6Al-4V oxide layer cross sections after heat-treatment at 900°C in ambient atmosphere: (a) 18 hours; full cross section (b) 48 hours; upper region (c) 48 hours; full cross section (d) 60 hours; full cross section (blue= titanium and red= aluminium).

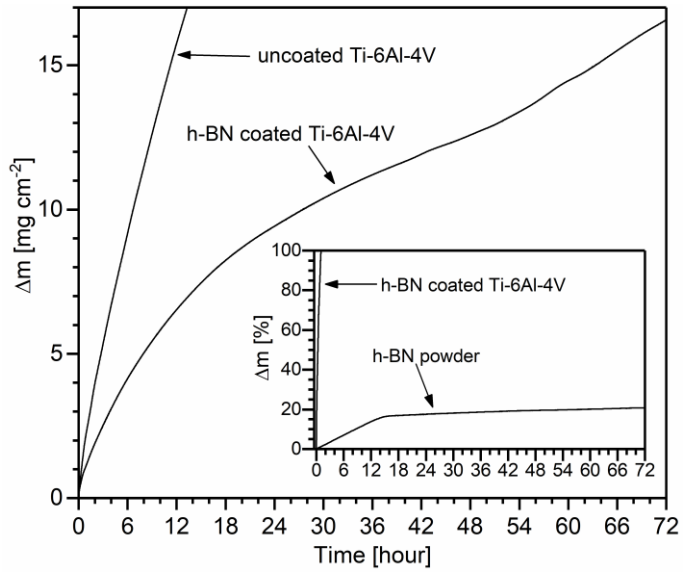

Figure 12. TGA plots from samples that were exposed to a dry 80% N_2: 20% O_2 atmosphere for 72 hours at 900°C. Main figure shows h-BN coated Ti-6Al-4V and uncoated Ti-6Al-4V. The mass gain for each is normalised to unit surface area of the substrate. Inset shows h-BN coated Ti-6Al-4V and the isolated coating. With the mass of the substrate having been several orders of magnitude greater than that of the coating, the ordinate is expressed as a percentage of the initial mass of h-BN. Due to considerable Δm differences, to aid clarity only the early stage of exposure is shown for one of the two traces in each plot.

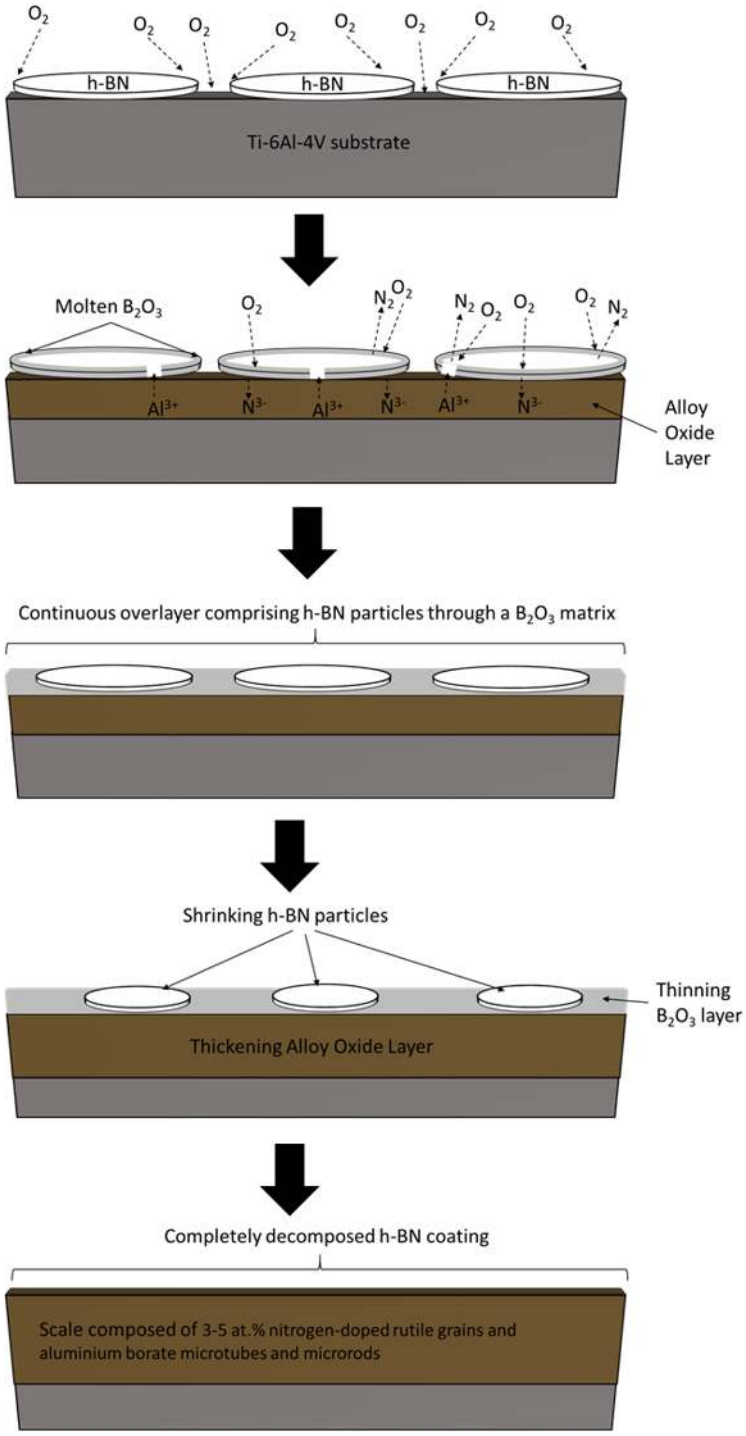

Figure 13. Schematic of the proposed reaction mechanisms that lead to complete decomposition of an h-BN coating on Ti-6Al-4V in ambient atmosphere at 900°C. To aid clarity, only a single layer of h-BN is shown and the intergranular gaps have been exaggerated.

Table 1. Nominal wt.% composition of Ti-6Al-4V.

Ti	Al	V	Fe	C	N	O	H
Bal	5.5-6.75	3.5- 4.5	<0.25	<0.08	<0.05	<0.2	<0.0125

Graphical Abstract

Ti-6Al-4V forming is a key manufacturing process that typically employs a hexagonal boron nitride coating as a lubricant/release agent. In air at 900°C, the substrate and coating undergo concurrent and interrelated high temperature oxidation. This results in complete decomposition of the coating and a radically altered scale outer-interface comprising aluminium borate and nitrogen-doped rutile.